

On the Red Edge of the δ Scuti Instability Strip

Yan Xu ^{1,2*}, Zhi-Ping Li ¹, Li-Cai Deng ¹ and Da-Run Xiong ³

¹ National Astronomical Observatories, Chinese Academy of Sciences, Beijing 100012

² Department of Physics, Tianjin Normal University, Tianjin 300073

³ Purple Mountain Observatory, Chinese Academy of Sciences, Nanjing 210008

Received 2002 June 17; accepted 2002 July 24

Abstract The δ Scuti star catalogue is used to derive the observational locations of such stars on the HR diagram. The theoretical and observational instability strips are compared to check the theoretical red edge obtained by considering non-local time-dependent convection theory. The observational instability strip almost overlaps with the theoretical one, but the observed blue and red envelopes are hotter than the theoretical edges. The distribution of δ Scuti stars in the pulsation strip is not uniform.

Key words: stars: variables: δ Sct — stars: oscillations — stars: HR diagram

1 INTRODUCTION

δ Scuti stars, a type of small amplitude variables, are located in the intersection region between the cepheid instability strip and the main sequence. Their spectral types range from A to F. Most of them belong to Population I. Most of δ Scuti stars pulsate with periods from 0.02 to 0.25d (Breger 2000). Pulsating stars provide important diagnosis for stellar interior structure and evolution. Similar to most other types of pulsating variables, the δ Scuti variables are driven by the κ mechanism: during each cycle the kinetic energy of pulsation is supplied by the internal energy of the mixture of gas and radiation in the ionization zones (Breger 2000).

Previous pulsation strip was presented by Pamyatnykh (2000) and Breger (1979). These theoretical models only predicted the blue edge of the instability strip while the red edge could not be obtained due to the lack of a valid time-dependent theory of convection to deal with the coupling between pulsation and convection. So only empirical red edge was discussed in those papers.

Xiong & Deng (2001) set up a non-local, time-dependent statistical theory of convection (Xiong et al. 1989) and obtained the theoretical red edge. The δ Scuti stars are low mass stars ranging from $1.5 M_{\odot}$ to $2.5 M_{\odot}$. Near the blue edge, the surface convective zone is very shallow, so convection has no significant effect on the oscillation of these blue stars. In the course of evolution, the convective zone penetrates deeper and deeper, and convection becomes more and

* E-mail: xuyan@ns3.bao.ac.cn

more important for the pulsation, until it becomes the most significant factor for the existence of the red edge. Convection influences pulsation through three factors, namely convective energy transfer (thermodynamic coupling), turbulent pressure and turbulent viscosity (dynamic coupling). Turbulent viscosity is always a pure damping factor, whereas turbulent pressure is, in general, an excitation mechanism for stellar pulsation. Thermodynamic coupling has a damping effect in the deep layer of convective zone but it has an excitation effect at the top of the convective zones. These three factors contribute differently to pulsation with different stellar structures and pulsation modes. This fact can explain the complex pulsational character in different regions of the HR diagram (Xiong & Deng 2001).

In the present paper we compare the observational δ Scuti pulsation strip and the theoretical result in order to examine the theoretical red edge obtained by Xiong and Deng (2001). Section 2 introduces the process of relating the photometric parameters to the theoretical framework of the HR diagram in our way toward our goal. We then compare the theoretical and observational edges of the pulsation strip. Section 3 discusses stars with unusual locations on the HR diagram, and possible reasons for discrepancies between the theory and observations.

2 INSTABILITY DOMAIN DELIMITED BY THEORY AND OBSERVATION

2.1 Calculation with Calibration of $wvby$ β Photometry

Our observational data are taken from the revised δ Scuti stars catalogue compiled by Rodriguez et al. (2000). This catalogue lists 636 variables, of which 323 have available $wvby\beta$ photometry and their β values are in the range $2.60 < \beta < 2.93$. Among them, 20 stars beyond the slope of δc required by calibration were discarded ($\delta c < 0.2$ for stars with $\beta < 2.63$ and $\delta c < 0.28$ for stars with $2.63 < \beta < 2.88$). So, a total of 303 stars are used in our work. Because the main source of information for Strömberg photometry comes from the catalogue of Hauck & Mermilliod in 1998 (Rodriguez 2000), the accuracy of the original photometric data can be estimated from the data of the $wvby - \beta$ Catalogue (Hauck et al. 1998). There are 209 δ Scuti stars included in this catalogue. 54 stars have intact photometric data $b - y$, c_1 , m_1 , β , V and their errors. In the catalogue, observational data from different sources are used to obtain final weighted mean values and their errors. The average errors of the photometric indices are: $e(\beta) = 0.0062$, $e(c_1) = 0.0067$, $e(b - y) = 0.0033$, $e(m_1) = 0.0051$, $e(V) = 0.0099$

The effective temperature and absolute magnitude are the fundamental parameters for the HR diagram. Reddening correction is applied to the photometric data and the absolute V magnitude is calculated using calibration (Crawford 1975, 1979). In the calculation, stars are divided into several groups according to their β index and the different groups are calibrated with different empirical relations.

For F-type stars with $2.6 < \beta < 2.72$, all the color indices except β suffer from extinction. β is the key data in the calculation of $(b - y)_0$ and $E(b - y)$. After these, the intrinsic color indices can be obtained according to the relations $E(b - y) = 0.73E(B - V)$, $E(m_1) = -0.3E(b - y)$ and $E(c_1) = 0.2E(b - y)$. The differences between the observational indices and the standard values given by the standard relations for the Hyades cluster (Crawford 1975), are $\delta m = m_1$ (standard) $- m_1$, $\delta c = c_1 - c_1$ (standard). The absolute V magnitude can be calculated using $M_v = M_{ZAMS} - f \times \delta c$ (Crawford 1975), where $f \times \delta c$ represents the effect of evolution. The initial T_{eff} can be found by the relation of $T_{\text{eff}} = 5040 / (0.771453 \times (b - y)_0 + 0.546544)$.

For F-type stars and A-type stars with $2.72 < \beta < 2.88$, their calibrations follow the same principle, but they have different initial parameters and empirical relations.

Usually $(u - b)_0$ is a measure for T_{eff} for early-type stars and $(b - y)_0$ is one for late-type stars. So for the intermediate type, a linear combination of $(u - b)_0$ and $(b - y)_0$ is adopted. In the same way, as β is an indicator of M_v for the early group and $[c1]$ for the late group, a linear combination of β and $[c1]$ is used for the intermediate group (Strömgren 1966).

For the A-type stars with $2.87 < \beta < 2.93$, which are located in this region, the parameters a_0 and r , defined as follows, are used to calibrate their absolute magnitudes and initial effective temperatures, instead of using $(b - y)_0$ and $[c1]$,

$$a_0 = (b - y)_0 + 0.18((u - b)_0 - 1.36),$$

$$r = (\beta - 2.565) - 0.35[c1].$$

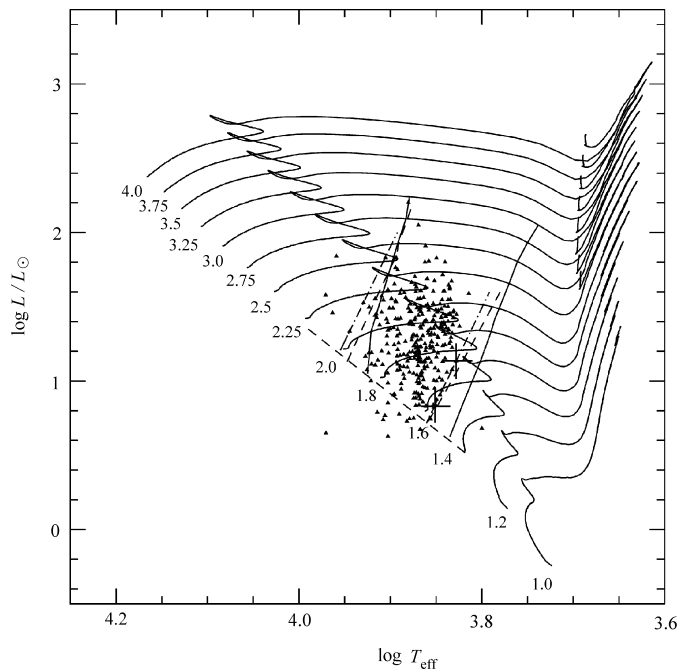


Fig.1 Triangles represent the observational points whose luminosities are obtained through calibration. Dot-dashed lines are the envelopes of the observational pulsational strip. Solid lines represent the theoretical blue and red edges given by Xiong and Deng (2001). The dashed lines represent the theoretical blue edge, empirical red edge and the ZAMS given in (Pamyatnykh 2000). The average error bar is marked on two stars near the red edge.

The intrinsic color index and initial effective temperature are used to obtain more accurate values of T_{eff} and $\log g$ by using grids calculated from models of stellar atmosphere (Moon & Dworetzky 1985). The bolometric correction (BC) for a given star is interpolated from its T_{eff} and $\log g$. The final result is shown in Fig.1. The observational points are represented by triangles and their envelopes defining the pulsational strip, by dot-dashed lines, outliers having been excluded. The average error bars for $\log T_{\text{eff}}$ and $\log L/L_{\odot}$ are marked on two stars near the

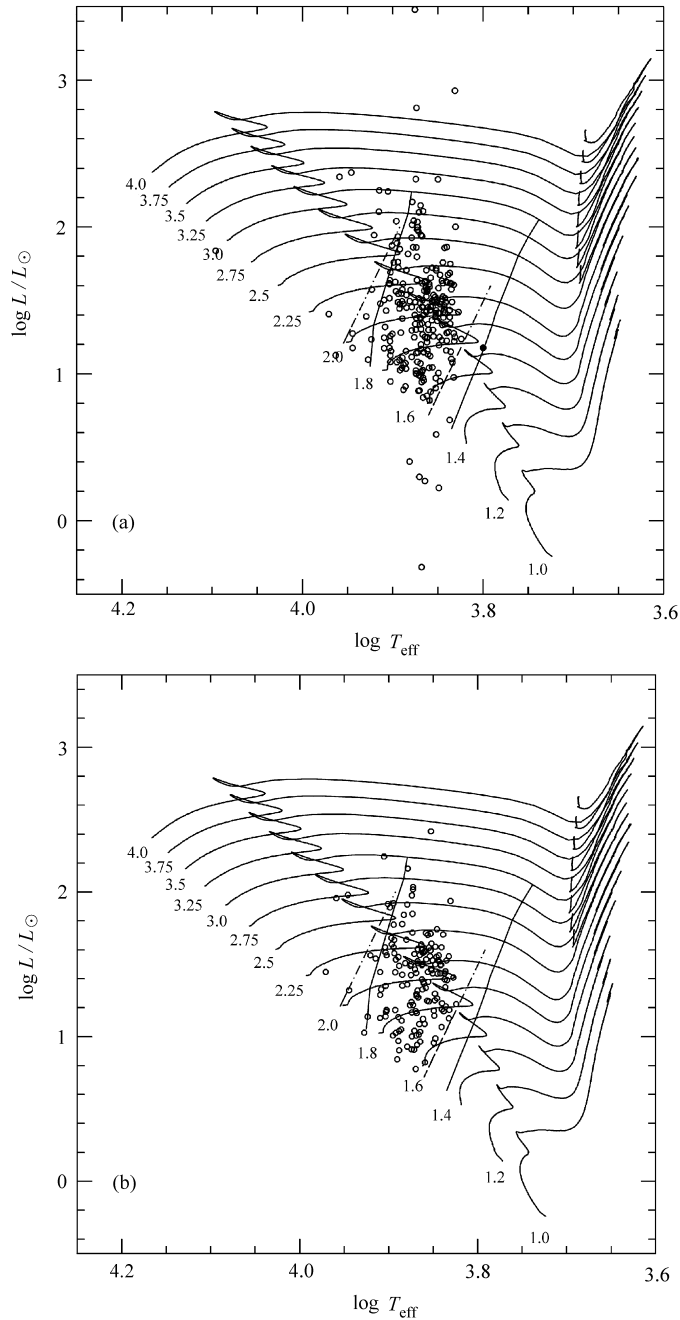


Fig. 2 a) Circles are observational points with luminosities obtained by using their parallaxes. All the stars in catalogue having available parallaxes and color indices are plotted. Solid lines represent the theoretical blue and red edges from Xiong & Deng (2001). Dot-dashed lines are the same as those in Fig. 1. b) Same as Fig. 2a but restricted to stars with relative errors of parallax less than 0.2.

red edge. Uncertainty in $\log L/L_{\odot}$ was made by Breger (1990). The observational uncertainties of β and c_1 , assumed to be mutually independent, are estimated from normal distributions of errors. It is assumed that the BC is too small to affect the uncertainty. It is concluded that M_v has a typical error of ± 0.3 mag for A-type stars and ± 0.25 mag for F-type stars. It then follows that the uncertainty $\log L/L_{\odot}$ is about ± 0.12 . Uncertainty in effective temperature obtained from atmosphere models was estimated by Moon & Dworetzky (1985). The mean difference between values of T_{eff} determined from the grids and the fundamental values is -10 K with a systematic error ± 260 K.

2.2 Calculation of M_v with Parallax

Because most of δ Scuti stars have Hipparcos parallaxes available, it is possible to check the observational pulsational strip with another method. The observational points derived from the parallaxes are plotted in Fig. 2. All stars with available parallaxes are plotted in Fig. 2a and stars with relative errors in parallax more than 20% are excluded in Fig. 2b. The same restriction was used by Rodriguez & Breger (2001) which corresponds to an error of 0.43^{m} in $M_v(\pi)$. There are 252 stars plotted on Fig. 2a, of these 65 stars have relative errors more than 20%.

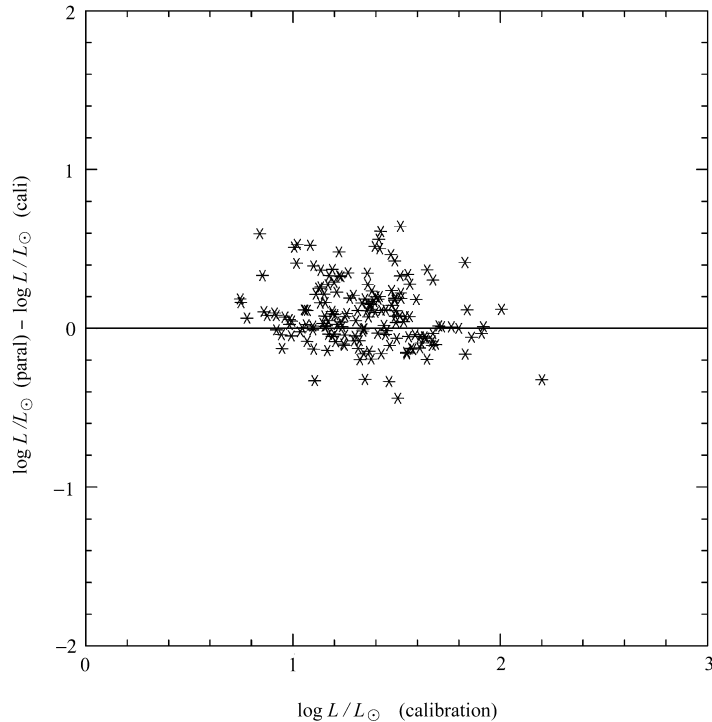


Fig. 3 Comparison of the luminosities obtained in two different ways.

Parallax and visual V magnitude are used to get the absolute V magnitude, after applying an interstellar extinction according to the empirical formula $V_0 = V - 4.3E_{b-y}$ (Rodriguez & Breger 2001; Crawford 1976). BC is obtained by interpolating the BC table (Cox 1999). Temperature is obtained as described in Section 2.1.

The luminosities obtained in the two different ways are compared in Fig. 3. The average value of $\log L/L_\odot$ derived from the parallaxes is 0.0912 higher than that from the calibration, or 0.228 mag brighter. The rms of difference in $\log L/L_\odot$ is 0.22, but this is not a critical factor for the location of the pulsational strip. The previous envelopes obtained by calibration are drawn in Fig. 2 with dot-dashed lines. We see that the pulsational strips given by the two methods overlap each other. In Fig. 2a there are some stars below the ZAMS or above the normal region. These stars are checked and most of them show some peculiarity. They are discussed in Section 3.

2.3 Theoretical and Observational Instability Domains

In order to compare the theoretical red edge with the observational red edge, the theoretical pulsational strip and the observed δ Scuti stars are plotted in the HR diagram (Fig. 1). The theoretical pulsational strip and evolutionary tracks shown in solid lines are calculated by Xiong & Deng (2001). The dash lines mark the ZAMS, theoretical blue edge and the empirical red edge, given in Pamyatnykh (2000). Triangles represent the observational points, and dot-dash lines mark their envelopes. Points far away from the pulsational strip are not included. It is found:

Blue Envelope: $\log T_{\text{eff}} = 3.955$ on the ZAMS, $\log T_{\text{eff}} = 3.892$ at $\log L/L_\odot = 2$

Red Envelope : $\log T_{\text{eff}} = 3.86$ on the ZAMS, $\log T_{\text{eff}} = 3.792$ at $\log L/L_\odot = 1.6$

The theoretical blue edge and empirical red edge given by Pamyatnykh (2000) and shown in Fig. 1 are hotter than the theoretical edges given by Xiong and Deng (2001) near the ZAMS. At relatively high luminosity, the blue edges fit well with each other.

The observed blue envelope is about 200 degree hotter than the blue edge obtained by Pamyatnykh (2000). The observational points fit well with the empirical red edge (Pamyatnykh 2000).

The theoretical red edge (Xiong & Deng 2001) approximately agrees with the observational red envelope curve at relatively high luminosity, but there are some difference near the ZAMS. At luminosity 0.84, there is a temperature difference of about 400 K between them.

The distribution of δ Scuti stars in the pulsational strip is not uniform. The observational points are mostly concentrated in the central region of the strip. There is a blank space at the relatively high luminosity region near the red edge. This may be caused by a large disparity in the proportion of MS to post-MS stars. In the region near the blue edge and the ZAMS, stars are sparse, maybe because hot dwarfs near the ZAMS are pulsating with high order p modes pumped by the atmosphere. The phenomenon support Xiong and Deng's theoretical blue edge which does not cover this region. But it does not get rid of the possibility that the amplitudes of these stars are so small that they have not been detectable (Xiong & Deng 2001).

The coolest star in the diagram is HD60987, with a fairly large value of $b - y = 0.299$ and a small $\beta = 2.64$. It is on the edge of the slope in which calibration is effective. The position of this star is not reliable, because it is far away from the red edge of the pulsational strip (Rodriguez & Breger 2001). The result of calculation based on its parallax is that this star is on the theoretical red edge. It is marked by a filled circle in Fig. 2a. The parallax of this star has a relative error of 0.206. So it was not included in Fig. 2b.

3 DISCUSSION

There are 12 stars below the ZAMS in Fig. 1. These stars and their color indices are listed in Table 1. It is obvious that all of these stars are in the range $2.72 < \beta < 2.88$. These stars do not show any peculiarity. Moreover, all of these stars are redistributed in the normal region of the pulsational strip when their parallaxes are used to calculate the magnitudes.

The stars below the ZAMS in Fig. 2a are listed in Table 2. These are all completely different from those of Table 1. Except HD183324 which is a very metal-poor star and has a very small amplitude 0.004 mag, the rest have amplitudes larger than 0.3 mag. When the amplitude is large, it may be difficult to determine the mean V magnitude accurately. Stars in Fig. 2a with $\log L/L_{\odot} > 2.2$ are listed in Table 3. These are five metal poor stars (HD79889, HD11956, HD153747, HD214698 and HD218549), one spectroscopic binary (HD191747). And there are four large amplitude stars. The main reason for the unusual position of these stars is the large parallax error.

Table 1 Parameters of Stars below the ZAMS in Fig. 1

ID name (1)	$b - y$ (2)	$m1$ (3)	$c1$ (4)	β (5)	$\log(L/L_{\odot})$ (6)	T_{eff} (7)	Type (8)
HD 3326	0.171	0.217	0.731	2.783	0.745280	7570	A5m
HD 13079	0.203	0.211	0.672	2.759	0.675938	7370	F0
HD 13038	0.105	0.220	0.848	2.856	0.789564	8210	A5V
AB Cas	0.252	0.137	0.789	2.829	0.628369	7990	A3V+K1V
HD 21553	0.167	0.174	0.939	2.872	0.999681	8340	A6Vn
HD 23156	0.151	0.202	0.823	2.837	0.766770	8050	A7V
HD 23567	0.229	0.173	0.748	2.788	0.730240	7620	A9V
HD 23607	0.153	0.188	0.823	2.841	0.739908	8090	A7V
2362-16	0.060	0.155	0.694	2.787	0.649745	9340	
HD 71935	0.142	0.197	0.906	2.780	0.852496	7990	A9-F0III-I
BP Peg	0.228	0.161	0.857	2.775	0.777520	7770	A5-F0
HD 209775	0.189	0.219	0.718	2.774	0.749084	7490	F0

Table 2 Parameters of Stars below the ZAMS in Fig. 2a

ID name (1)	$b - y$ (2)	$m1$ (3)	$c1$ (4)	β (5)	$\log(L/L_{\odot})$ (6)	T_{eff} (7)	Parallax (error) (8)	Type (9)
GP And	0.185	0.146	0.842	2.766	-0.315862	7380	9.22 (4.25)	A3
HD 64191	0.185	0.180	0.854	2.760	0.269441	7320	8.40 (1.73)	F0III
CW Ser	0.222	0.169	0.854	2.733	0.223040	7060	2.77 (3.40)	A-F
DY Her	0.217	0.181	0.821	2.738	0.587238	7110	6.51(1.91)	F4III
HD 183324	0.051	0.167	1.002	2.890	1.125661	9190	16.95(0.87)	λ

That the theoretical red edge is cooler than the observational red envelope near the ZAMS may be explained as follows. Metal abundance seriously affects the location of the red edge of the pulsational instability strip. For the same effective temperature, stars with poorer metal abundance have shallower convective zones. The existence of the red edge is due to the convective zone extending below the ionization zone and the pulsation being damped. So for arriving at the same convective depth, the red edge given by stars of poorer metal abundance will move

to the right. Using a model of richer metal abundance will fit the observations better. Another very possible reason is that in the lower part of the pulsational strip, the location of the red edge depends sensitively on the convective parameter. It is possible that theoretical value is smaller than the real value. On the other hand, the data of δ Scuti stars in the catalogue is collected from various sources, they have different observational uncertainties and different systematic errors. The errors in the observed positions can be attributed to such uncertainties.

Table 3 Parameters of Stars having Abnormally High Luminosities in Fig. 2a

ID name (1)	$b - y$ (2)	$m1$ (3)	$c1$ (4)	β (5)	Type (6)	$\log(L/L_{\odot})$ (7)	T_{eff} (8)	parallax (error) (9)
HD 11956	0.094	0.169	1.123	2.840	A5V	2.241540	8300	3.37 (0.58)
HD 20919	0.207	0.178	0.765	2.775	A8V	2.325836	7450	1.18 (1.45)
HD 79889	0.160	0.159	0.841	2.780	A3	3.478995	7560	0.36 (1.15)
HD 153747	0.098	0.136	1.034	2.859	A0III	2.248444	8360	5.32 (0.98)
HD 191747	0.045	0.170	1.143	2.895	A3III	2.370358	8960	7.77 (0.65)
DELac	0.317	0.154	0.779	2.703	F6	2.926340	6950	0.20 (1.84)
HD 214698	0.014	0.155	1.144	2.872	A2V	2.340165	9040	5.13 (0.77)
HD 218549	0.210	0.129	0.872	2.777	A6	2.810195	7560	0.36 (2.02)
HD 223338	0.198	0.154	0.861	2.736	F0	2.323030	7280	0.81 (1.59)

Acknowledgements This paper is supported in part by the National Natural Science Foundation of China (NSFC) through grant 10173013 and by the Ministry of Science and Technology of China through grant G19990754. XDR thanks NSFC for continuous support.

References

- Breger M., 1979, PASP, 91, 5
Breger M., 2000, In: Breger M., Montgomery M. H. eds., ASP Conf. Ser. Vol. 210, Delta Scuti and Related Stars, p.3
Breger M., 1990, In: Confrontation between stellar pulsation and evolution, Proceedings of the Conference, San Francisco, CA, Astronomical Society of the Pacific, 1990, p.263
Cox A. N., 1999, Allen's Astrophysical Quantities, 388
Crawford D. L., Mandwewala N., 1976, PASP, 88, 917
Crawford D. L., 1975, AJ, 80, 955
Crawford D. L., 1979, AJ, 84, 1858
Hauck B., Mermilliod M., 1998, A&AS, 129, 431
Moon T. T., Dworetzky M. M., 1985, MNRAS, 217, 305
Pamyatnykh A. A., 2000, In: Breger M., Montgomery M. H. eds., ASP Conf. Ser. Vol. 210, Delta Scuti and Related Stars, p.215
Rodriguez E., Lopez-Gonzalez M. J., Lopez de Coca P., 2000, A&AS, 144, 469
Rodriguez E., Breger M., 2001, A&A, 366, 178
Strömberg B., 1966, ARA&A, 4, 433
Xiong D. R., 1989, A&A, 209, 126
Xiong D. R., Deng L., 2001, MNRAS, 324, 243